HHS Public Access

Author manuscript

Gastroenterology. Author manuscript; available in PMC 2020 May 01.

Published in final edited form as:

Gastroenterology. 2019 May ; 156(6): 1834–1848. doi:10.1053/j.gastro.2019.01.041.

PRC2 proteins EZH1 and EZH2 Regulate Timing of Postnatal Hepatocyte Maturation and Fibrosis by Repressing Gene Expression at Promoter Regions in Euchromatin in Mice

Jessica Mae Grindheim[1,2,3,4,5], **Dario Nicetto**[1,2,3], **Greg Donahue**[1,2,3,5], and **Kenneth S Zaret**[1,2,3,5,6,#]

[1]Institute for Regenerative Medicine, University of Pennsylvania, Smilow Center for Translational Research, 3400 Civic Center Blvd, Bldg. 421, Philadelphia, PA 19104-5157, USA.

[2]Penn Epigenetics Institute, University of Pennsylvania, Smilow Center for Translational Research, 3400 Civic Center Blvd, Bldg. 421, Philadelphia, PA 19104-5157, USA.

[3]Dept. Cell and Developmental Biology, University of Pennsylvania, Smilow Center for Translational Research, 3400 Civic Center Blvd, Bldg. 421, Philadelphia, PA 19104-5157, USA.

[4]Dept. of Cancer Biology, University of Pennsylvania, Smilow Center for Translational Research, 3400 Civic Center Blvd, Bldg. 421, Philadelphia, PA 19104-5157, USA.

[5]Perelman School of Medicine, University of Pennsylvania, Smilow Center for Translational Research, 3400 Civic Center Blvd, Bldg. 421, Philadelphia, PA 19104-5157, USA.

[6]Lead contact

Abstract

BACKGROUND & AIMS: Little is known about mechanisms of postnatal hepatocyte maturation or chromatin regulation of genes that control fibrogenesis. We investigated transcription of genes that regulate fibrosis and the effects of chromatin compaction and the polycomb repressive complex 2 (PRC2) in postnatal hepatocytes of mice, focusing on the roles of the histone methyltransferases EZH1 and EZH2.

METHODS: Hepatocytes were isolated from C57BL/6J and C3H mice, as well as mice with liver-specific disruption of *Ezh1* and/or *Ezh2*, at postnatal day 14 (P14) and 2 months after birth (M2). Liver tissues were collected and analyzed by RNA-seq, H3K27me3 chromatin

[#]**Correspondence:** Kenneth S Zaret, Ph.D. 3400 Civic Center Blvd., Rm. 9-132 Philadelphia, PA 19104-5157. zaret@pennmedicine.upenn.edu. Office: 215-573-5813.

Author contributions: Conceptualization, J.M.G. and K.S.Z.; Investigation, J.M.G, D.N.; Formal Analysis, J.M.G, G.D.; Data Curation, J.M.G. and G.D.; Writing, J.M.G. and K.S.Z.; Resources, K.S.Z.; Supervision, K.S.Z.; Funding Acquisition, J.M.G. and K.S.Z.

Disclosures: No competing interests to declare.

Transcript profiling: RNA-seq, srHC-seq, and H3K27me3 ChIP-seq data is available on NCBI GEO GSE119219. Results are additionally summarized in Supplementary Tables as a resource datasets. Further information, code, and requests may be directed to and will be fulfilled by the lead contact, Ken Zaret (zaret@pennmedicine.upenn.edu).

immunoprecipitation-seq, and sonication-resistant heterochromatin-seq (a method to map heterochromatin) analyses. Liver damage was characterized by histologic analysis.

RESULTS: We found more than 3000 genes differentially expressed in hepatocytes during P14 to M2 liver maturation. Disruption of *Ezh1* and *Ezh2* in livers caused perinatal hepatocytes to differentiate prematurely and express genes at P14 that would normally be induced by M2. This resulted in liver fibrosis. Genes with H3K27me3-postive and H3K4me3-positive promoter regions in euchromatin were prematurely induced in hepatocytes with loss of EZH1 and EZH2—these genes included those that regulate hepatocyte maturation, fibrosis, and genes not specifically associated with the liver lineage.

CONCLUSIONS: The PRC2 proteins EZH1 and EZH2 regulate genes that control hepatocyte maturation and fibrogenesis and genes not specifically associated with the liver lineage by acting at promoter regions in euchromatin. EZH1 and EZH2 thereby promote liver homeostasis and prevent liver damage. Strategies to manipulate PRC2 proteins might be used to improve hepatocyte derivation protocols or developed for treatment of patients with liver fibrosis.

Graphical Abstract

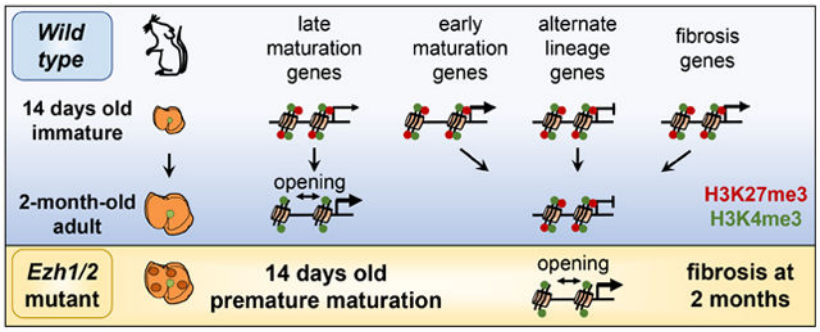

Keywords

epigenetics; hepatocyte; H3K27me3; fibrosis

Due to the shortage of fully differentiated cells for transplantation and disease modeling of various tissue types, there is interest in generating replacement cells. Directed differentiation and cell reprogramming can generate early stage cells, but with a failure to activate a terminally differentiated transcriptional program and a failure to repress genes of the starting cell type[1-4]. In directed differentiation of hepatocyte-like cells, many fetal genes can be activated, but often there is failure to induce mature CYP P450 enzymes and repress fetal markers such as *Afp*[5-9]. When fibroblasts are reprogrammed to hepatic cells, the cells express liver markers and perform some liver metabolic functions but fail to activate various mature liver genes and cannot consistently rescue liver damage[10-12] The literature on embryonic liver development[13,14] rarely covers postnatal hepatic maturation[15-17], though there are major physiological changes in liver size, diet[18], microbiota and microbial metabolites[19,20], sexual maturation, and polyploidization[21]. Thus, there is a need to understand postnatal hepatic maturation.

Components of Polycomb Repressive Complexes 1 or 2 (PRC1 or PRC2) regulate multiple gastrointestinal cell types. The PRC2 protein EED promotes intestinal stem cell proliferation and inhibits differentiation[22], while the PRC1 protein BMI1 regulates intestinal stem cell proliferation and renewal[23(p1)]. PRC1 proteins BMI1 and MEL18 contribute to colitis-associated cancer[24]. PRC2 protein JARID2 is needed for late differentiation of pancreatic beta-cells[25]. In liver development, EZH2, one of the two H3K27me3 histone methytransferases, modulates the cell fate choice of embryonic endoderm to become pancreatic or hepatic buds [26] and is required for hepatoblast proliferation[27]. Loss of both EZH1 and EZH2 leads to chronic liver damage in adult mice[28]. Genes marked by the PRC2 repressive histone modification H3K27me3 exhibit activation defects in human fibroblast-to-hepatocyte reprogramming protocols, with genes in heterochromatin being the most resistant to activation[29-33]. This leaves open a role for Polycomb-based regulation in postnatal hepatic maturation.

By genetically ablating both *Ezh1* and *Ezh2*, we investigated the relationship between postnatal transcriptional, H3K27me3, and chromatin compaction dynamics in postnatal hepatocyte maturation and homeostasis. We found that PRC2 represses three main classes of genes in postnatal hepatocytes; hepatic maturation genes, non-liver lineage genes, and fibrosis genes. Genes that derepress in response to *Ezh1/2* loss have a unique chromatin signature. These findings impact our understanding of the means by which hepatocytes mature postnatally, how hepatocyte lineage fidelity is maintained, and how fibrosis genes are primed for a transcriptional response.

Results

Postnatal hepatic maturation involves differential expression of thousands of genes

Using RNA-seq on hepatocytes isolated by liver perfusion, we found 1215 upregulated and 2011 downregulated genes in hepatic maturation between P14 and M2 (alpha ≥ 0.05, FC ≥ 2) (Figure 1A, Supplementary Figure 1A-D, Supplementary Table 2,3,4). Upregulated genes include the key liver metabolic enzymes *Ces1f* and *Ces3b*, and are enriched by Gene Ontology for the Uniprot liver tissue expression category, P450 enzymes, and genes for metabolism of retinol, xenobiotics, and bile acids (Figure 1AB, Supplementary Table 5). As expected, fetal liver genes *Afp* and *Gpc3* are among the top downregulated genes (Figure 1A)[16,34]. Downregulated maturation genes enrich cell cycle, cell adhesion, differentiation, and signaling categories (Figure 1B). The cell cycle-associated categories reflect diminished proliferation in adult hepatocytes, as assayed by staining for proliferation marker PCNA (Supplementary Figure 1E). PubMed searches for a random sampling of genes in the cell adhesion and signaling categories and “liver” or “hepatocyte” often return no results, indicating that these may be new targets to study in liver maturation. Thus, P14 hepatocytes are transitioning extensively from a fetal to a mature transcriptional program.

P14 and M2 H3K27me3 states correlate with postnatal hepatic maturation

We profiled H3K27me3 in P14 and M2 hepatocytes (Supplementary Table 2,3). As expected, H3K27me3 was absent from the expressed liver gene *Alb* and present at the silent *Hoxd* cluster, and this anticorrelation of expression and H3K27me3 was observed genome-

wide (Supplementary Figure 1FG). H3K27me3 genomic coverage increased from 608 MB at P14 to 827 MB at M2 (Supplementary Figure 1H).

We called promoters and gene bodies as “lacking”, “losing”, “gaining”, or “retaining” H3K27me3 from P14 to M2. Acquisition of H3K27me3 is characteristic of many genes that are downregulated in the maturation transition from P14 to M2, with 44% of such promoters gaining (n=179) or retaining (n=909) H3K27me3 and 40% gene bodies gaining (n=172) or retaining (n=821) H3K27me3 (Figure 1C). In the case of gene bodies that retain H3K27me3, the percent of coverage increases from a median of 62% at P14 to 78% at M2; thus increasing H3K27me3 presence at these “retain H3K27me3 genes” was not discernible in categorical lack/lose/gain/retain calls (Figure 1D). This increase was not solely due to increased H3K27me3 coverage in M2 (p-value at 0.001, Monte Carlo simulation). About 9.4% (140) of promoters and 8.6% (129) of gene bodies belonging to maturation upregulated genes lose H3K27me3 during the P14 to M2 transition (Figure 1C). The H3K27me3 and transcriptional dynamics between P14 and M2 indicate a role for PRC2 proteins in regulating maturation gene expression.

EZH1 and EZH2 restrain premature postnatal hepatic maturation

To assess the role of PRC2 repression in postnatal hepatocytes, we performed RNA-seq on *Alb-Cre/Alb-Cre*; *Ezh1*$^{-/-}$; *Ezh2*$^{fox/flox}$ (“*Ezh1/2*”) hepatocytes, in which both histone methyltransferases for H3K27me3 are ablated. Loss of *Ezh1* or *Ezh2* alone does not result in H3K27me3 loss (Supplementary Figure 2A). *Ezh1* single knockout have transcriptomes highly similar to *Wt*, with only 203 differentially expressed genes (Supplementary Figure 2B, Supplementary Tables 2, 3). With a homozygous *Alb-Cre* transgene, whose expression starts around birth, P14 is the earliest age we observed quantitative H3K27me3 loss in *Ezh1/2* hepatocytes; hence this time was used to minimize secondary effects (Supplementary Fig 2CD). Notably, P14 *Ezh1/2* hepatocytes have expression profiles between *Wt* hepatocytes P14 and M2 hepatocytes (Supplementary Figure 1D). Strikingly, of the 1215 genes upregulated during hepatocyte maturation at M2, 263 (22%) are prematurely upregulated in P14 *Ezh1/2* hepatocytes (Figure 3A, Supplementary Table 3). Of the 2011 genes downregulated in hepatocyte maturation, 128 (6.3%) are prematurely downregulated in P14 *Ezh1/2* hepatocytes. Expression changes do not preferentially affect zonated genes (Supplementary Figure S2E). Taken together, the results indicate that the PRC2 proteins EZH1/2 normally restrain maturation of postnatal hepatocytes until the appropriate postnatal time.

Non-hepatocyte lineage genes are derepressed in P14 *Ezh1/2* hepatocytes

There are 665 genes upregulated and 90 genes downregulated in P14 *Ezh1/2* hepatocytes that are not normally changed during P14 to M2 maturation (Figure 3A, Supplementary Table 3). Upregulated genes include many transcriptional regulators, DNA-binding factors, and genes expressed in non-liver tissues, but GO analysis did not reveal specific biological pathways that were deregulated (Supplementary Table 5). These data are consistent with work from others that Polycomb proteins broadly repress alternate lineage-specific identity regulators[35-38], but are insufficient upon deletion to result in outright hepatocyte identity change at this postnatal maturation stage.

A subset of maturation and alternative lineage genes are repressed by *EZH1/2*

As expected, given the repressive functions of PRC2, the 263 prematurely upregulated "late maturation" genes have high H3K27me3 at promoters and gene bodies at P14, but not at M2, as compared to genes only upregulated in maturation (Figure 2B). There are 148 genes upregulated in P14 *Ezh1/2* hepatocytes (Figure 2A), although they are normally downregulated in maturation and H3K27me3-marked, indicating that these are "early maturation" genes that are downregulated in the course of maturation by PRC2. The 665 "alternative lineage" genes upregulated in P14 *Ezh1/2* mutants have high P14 and M2 H3K27me3 levels and the majority are lowly expressed in *Wt* hepatocytes (Supplementary Figure 2H). These data support a model where PRC2/H3K27me3 repression is used to repress early and late maturation genes at the appropriate times and non-hepatocyte alternative lineage genes.

P14 and M2 H3K27me3 was low at liver enhancers, regardless of whether the enhancers were centered by DNase hypersensitivity or if windows were varied around enhancer centers from 200 bp to 5 kb (Supplementary Figure 2G). Specifically, H3K27me3 levels were low at enhancers associated with genes upregulated in P14 *Ezh1/2*, except for the early maturation genes, which had only 33 associated enhancers (Figure 2B). From this general lack of H3K27me3 at liver enhancers, we conclude that the *Ezh1/2* premature maturation phenotype is not functioning primarily through altered repression of enhancers.

In contrast, of the 263 prematurely upregulated maturation genes, 99 have P14 H3K27me3 at promoters and 85 have P14 H3K27me3 on gene bodies, for a total of 117 genes with at least one type of H3K27me3 marking. These genes include *Slc13a5*, which plays a key role in importing citrate into liver cells[39], *Pcsk9*, which is associated with liver cholesterol (LDL) uptake[40], and *Cyp26a1*, a key enzyme in the clearance of retinoic acid from the liver[41] (Figure 2C, Supplementary Figure 2F). In comparison, *Pax3*, a silent muscle gene, retains H3K27me3 marking at the promoter and was not upregulated in maturation. GO analysis on the 117 H3K27me3-marked genes did not reveal grouped biological process (data not shown). Taken together, we conclude H3K27me3 is used to restrain expression of genes in postnatal hepatocytes specifically at promoters and gene bodies, and minimally so at enhancers.

srHC-seq reveals that *Ezh1/2* sensitive genes have euchromatic and bivalently-marked promoters

To assess whether there are global changes in chromatin compaction in hepatic maturation, we characterized P14 and M2 *Wt* hepatocytes using an enzyme- and antibody-independent assay termed sonication-resistant heterochromatin sequencing (Supplementary Figure 3A). srHC-seq utilizes the physical property of crosslinked chromatin to be differentially sensitive to sonication; that is, structurally compact, heterochromatic regions are sonication-resistant while structurally open, euchromatic regions are sonication-sensitive[29] srHC-seq involves fractionation of large and small DNA fragments and analyzes the ratio of the two to identify both heterochromatic and euchromatic regions.

srHC-seq was highly reproducible in replicates (Supplementary Table 2, Supplementary Figure 3BC). We plotted srHC data as $\log_2$(large fragments/small fragments), with heterochromatic regions as y > 0 (Figure 3A, red) and euchromatic regions as y < 0 (Figure 3A, green). As expected, the silent, non-hepatocyte gene *Zfp936* has a heterochromatic profile in liver and genes at the highly expressed, hepatocyte-specific *Alb/Afp/Afm* locus have euchromatic profiles. Importantly, srHC-seq scores for promoters and gene bodies shows the inverse correlation between expression and chromatin compaction holds true genomically (Figure 3B).

In contrast to silent and highly expressed loci, *Cux2* expression is temporally- and sex-specific[42(p2)] and srHC profiles reflect these dynamics (Figure 3A). While sex-specific differences were ascertainable, the differences represent only a fraction of the genome. We therefore merged male and female srHC data for the remaining analyses.

Both P14 and M2 *Wt* hepatocytes have about 1200 Mb of srHC heterochromatin and 1100 Mb of euchromatin, with H3K27me3 occurring in both domains (Figure 3CD, Supplementary Figure 3DE). We did not observe a global increase of euchromatin in P14 *Ezh1/2* hepatocytes or by confocal microscopy of DAPI staining of 6-week-old *Ezh1/2* samples (data not shown). We conclude that large scale euchromatic and heterochromatic domains are generally stable in postnatal hepatic maturation, while a subset of genes are dynamic.

While the PRC2 complex is classically thought to repress expression by eliciting chromatin compaction[43], Polycomb-bound or -marked chromatin can be accessible to binding by some factors and transcribed[29,44-49]. PRC2 loss leads to derepression of only a fraction of H3K27me3-marked genes in diverse tissues, with promoter H3K4me2/3 predicting derepression[28,36,50]. To investigate the basis by which a subset of H3K27me3-marked promoters genetically respond to *Ezh1/2* loss, we plotted srHC-seq profiles at 8121 silent and 2221 highly expressed in P14 and M2 *Wt* animals (Figure 4A). Significantly, promoters of genes from all three classes of genes upregulated in P14 *Ezh1/2* hepatocytes are already euchromatic in P14 *Wt* hepatocytes, including those with promoter H3K27me3 signal (Figure 4A, note extensive green in P14 *Wt*). To focus on apparent direct PRC2 targets, we plotted srHC signal of genes with H3K27me3-marked promoters in P14 *Wt* samples (Figure 4B). These promoters become further euchromatic in *Ezh1/2* hepatocytes and the open regions increase in width (Figure 4B). Using published P12 liver ChIP data[51], we found that the three classes of P14 *Ezh1/2* upregulated genes have promoters with low levels of H3K4me3, RNA Polymerase II, and general transcriptional factors (Figure 4A, Supplementary Figure 4B).

By plotting signal at promoters of genes that are not differentially expressed in maturation or in P14 *Ezh1/2* hepatocytes and do have P14 promoter H3K27me3 (Figure 4A, “remaining P14 H3K27me3+ promoters”), we found that H3K4me3 does indeed help predict genes that become upregulated in *Ezh1/2* mutants, as does RNAP2, general TFs, and a pre-existing euchromatic chromatin state (Figure 4A, Supplementary Figure 4B). Thus, promoters that are open and poised yet restrained by PRC2 are regulated during hepatocyte maturation.

Chronic *Ezh1/2* loss leads to liver damage

It has previously been reported that *Ezh1/2* in liver leads to chronic liver damage and fibrosis in mice by 8 months and increased sensitivity to liver damaging agents[28]. We observe that apoptosis occurs 4.6-fold more in *Ezh1/2* hepatocytes by 1 month postnatal with very rare ductular reactions (Figure 5A). Yet by M2, but not at M1, liver fibrosis can be detected by Sirius Green/Fast Red staining (Figure 5B, Supplementary Figure 5A). Additionally, ductular responses can occur by H&E and CK19 staining by M2, with some larger diameter, malformed ducts than were reported previously (Figure 5B, Supplementary Figure 6A). Macroscopic regenerative nodules occur in nearly half of *Ezh1/2* livers by M2, visible in H&E sections or in the most severe cases, by the naked eye as lumps on the liver (Figure 5C). While the *Ezh1/2* model loses H3K27me3 in nearly 100% of hepatocytes at P14 (Supplementary Figure 2C), by M2 these nodules stain for H3K27me3 similar to *Wt* and also stain for EZH2 (Figure 5DE, Supplementary Figure 6AC), which was not observed previously in Bae et al.[28]. As the liver is a regenerative organ and nodular hepatocytes in *Ezh1/2* livers have increased proliferation (Supplementary Figure 6C), we conclude that the EZH2+ nodules originate by selection for rare cells which escape *Alb-Cre* recombination. Thus, loss of PRC2-based repression results in loss of hepatic homeostasis, chronic liver damage, and fibrosis.

Genes involved in liver fibrosis are primed by euchromatic H3K27me3+ promoters

A 232 gene signature predicting fibrosis before histopathological detection was identified using a non-alcoholic steohepatitis (NASH) mouse model, and the relevance to humans was confirmed by finding 71 of 123 human NASH genes in the mouse 232 gene datasets[52,53]. RNA-seq on liver biopsies from a mixed cohort of chronic liver disease patients with Hepatitis C and/or fatty liver disease identified 121 genes upregulated in advanced human liver fibrosis as compared to early fibrosis[54]. We found that genes from both datasets are normally downregulated in postnatal hepatic maturation, are upregulated in P14 and M2 *Ezh1/2* hepatocytes, and have the predictive euchromatic H3K27me3+/H3K4me3+ promoter chromatin state that we identified as sensitizing genes to *Ezh1/2* loss (Figure 6A). Genes significantly upregulated in P14 *Ezh1/2* samples in mouse and human datasets were each 2.6-fold more likely to have P14 H3K27me3+ promoters (permutation test, p=0.003 and p=0.009). Included in fibrosis gene sets with H3K27me3 promoter-marked genes are *Fbn1*, an inflammation and chemotaxis gene that is also upregulated in response to damaging chemicals[55], *Fstl1*, which is upregulated in humans with HCV-induced fibrosis and steatosis[56], and *Col1a1*, which is upregulated in mice and humans with liver fibrosis[57] (Figure 6B, Supplementary Figure 7BC). Interestingly, genes proposed to be involved hepatocyte epithelial-mesenchymal transition (EMT) in response to liver damage include *Tgfb1, Vim*, and *S100a4*58 also have H3K27me3-marked promoters and may be upregulated in M2 *Ezh1/2* hepatocytes (Figure 6B, Supplementary Figure 7BC). Together, the failure to repress fibrosis-related genes starting at two weeks postnatal is associated with the 2-month-old fibrotic phenotype in *Ezh1/2* livers.

Discussion

To be effective therapeutically, newly generated hepatocyte-like cells must perform the complex metabolic functions of native hepatocytes that are naturally induced postnatally[59-61], but these late maturational functions are limited in many hepatocyte-like cells[5-9]. Here we define a P14 to M2 transitional hepatocyte profile with more than 3000 transcripts exhibiting differential expression. The RNA maturation dataset can be a useful resource for assessing the stage of hepatocytes generated from stem cells or by directed reprogramming. Perinatal loss of EZH1/2 in hepatocytes leads to premature differentiation, suggesting that modulation of Polycomb components may enhance maturation in protocols for generating new hepatocytes.

In our study, altering PRC2 repression led to impaired liver function and fibrosis, and previous reports have shown impaired ability to respond to liver damaging agents[28]. Interfering with splicing factors alters liver maturation in mice and also leads to susceptibility to liver damage[15]. Considering the rising worldwide prevalence of NASH and hepatitis B[62] and that fibrosis is a key indicator of chronic liver injury of any etiology[63], the common thread of impaired maturation predisposing the adult liver to damage suggests that studying mechanisms of hepatic maturation may help us identify environmental factors that alter maturation in humans and predispose them to liver diseases. Here we have identified a H3K27me3+/H3K4me3+ euchromatic promoter signature that primes many genes to be upregulated in response to maturation or other signaling events, and we propose that this is a chromatin-level mechanism leading to liver fibrosis in the *Ezh1/2* model. Given the euchromatic state of these promoters, it may be that compaction-independent repressive activities of Polycomb proteins, such as PRC2 inhibiting elongation[66] and PRC1 interfering with RNAPII recruitment[64,65], are key to regulating transcription in postnatal hepatocytes, though a full catalog of precise mechanisms by which Polycomb proteins repress transcription is still being worked out. It will be interesting to see how agonists or antagonists of different aspects of Polycomb Protein function may help reverse fibrosis, considering that there is growing evidence of fibrotic reversal after treatment for hepatitis B, C, and autoimmune hepatitis[63].

There is conflicting evidence suggesting that hepatocytes can acquire a fibroblastic phenotype and expression of mesenchymal markers through EMT during liver fibrosis or in response to TGBβ treatment[58,67-69]. We find that expression of these mesenchymal markers is slightly upregulated in M2 *Ezh1/2* hepatocytes, but expression is highly variable (Supplementary Figure 6). This may reflect variability of multiple different sources, including variable levels of liver damage and fibrosis, variable contributions of H3K27me3+ nodular hepatocytes, and variable numbers of cells undergoing EMT at possibly different stages of EMT. The mesenchymal genes tend to be marked by H3K27me3 and have euchromatic promoters (Figure 6, Supplementary Figure 7). While we cannot conclude from these results whether EMT is occurring, it will be interesting to assess whether PRC2 repression maintains an epithelial state in hepatocytes by repressing mesenchymal genes and whether liver damage elicits their derepression.

Our results emphasize the role of PRC2 proteins in regulating maturation and how that may affect fibrosis, but not all maturation genes in our dataset are prematurely up- or downregulated in P14 *Ezh1/2* mutants. There must be other mechanisms that regulation maturation genes in response to changing diet, microbiota, and sexual maturation during the two week to two month period. These results highlight the need to identify maturation factors, both for the purposes of enhancing *in vitro* hepatic maturation and for understanding factors which predispose humans to disease.

Methods

Liver perfusion and hepatocyte isolation

Mice are anesthetized using isoflurane, the abdominal cavity exposed, venae cavae cannulated, and the portal vein severed. 37°C liver perfusion media (Invitrogen 17701-038) and then liver digest media (Invitrogen 17703-034) are perfused (25 mL for P14, 45 mL for M2). Dissociated livers in William's E are strained through a 100 μm filter (Figure S1a) and pelleted at 50g for 5 min at 4°C. Hepatocyte enrichment was confirmed by depletion of RNAs from contaminating cells types by comparing whole perfused liver, isolated hepatocytes, and supernatant (pelleted at 500g) fractions.

RTqPCR

RNA was isolated from TRIzol, cDNA generated (Biorad 170-8891), and expression analyzed with Power SYBR Green (Thermo 4368577).

Western blotting

Whole cells or nuclei (isolated by douncing in RSB) were resuspended in Buffer C (200 mM Tris pH 7.9, 400 mM NaCl, 1 mM EDTA, 1 mM EGTA, 0.8% SDS, PIC (Roche #11873580001), 1mM PMSF). Nuclear extracts were sonicated to reduce the viscosity from high DNA content. Extracts were denatured for 30 min at 99°C in 100mM DTT/Sample Buffer (Thermo NP0007) and run with the NuPAGE system (NP0335,NP0002) at 80V. Wet transfer to PVDF membranes (100V for 3 hr, transfer buffer NP0006) and membranes were blocked for an hour in 5% NFDM-TBST. Primary antibodies were incubated overnight in 5% NFDM-TBST. Secondary antibodies (Santa Cruz Biotechnology sc-2004, sc-2005) were incubated in 5% NFDM-TBST for 1 hour. Blots were developed using Thermo #34080. Primary antibodies: H3: 1/5000 Millipore 05-928. H3K27me3: 5ug/mL Abcam 6147. H3K27me3: 1/1000 Active Motif 39155.

Chromatin preparation and immunoprecipitation

Hepatocytes were fixed in 25 mL 1% formaldehyde in PBS for 10 min at room temperature, quenched with 2.3 mL 2.5 M glycine for 5 min, pelleted at 4°C at 50g for 5 min, resuspended in 10 (P14) or 20 mL (M2) ice-cold RSB (10 mM Tris pH7.4, 10 mM NaCl, 3 mM MgCl2, 0.5% NP40, PIC, 0.1 mM PMSF, 1% Triton-X 100), dounced, pelleted for 10 min at 4°C at 100g, and resuspended in 2 mL ice-cold AS sonicationlysis buffer (10 mM Tris-HCl, pH8, 100 mM NaCl, 1 mM EDTA, 0.5 mM EGTA, 0.1% Na-deoxycholate, 0.5% N-lauroylsarcosine, 1 mM DTT, PIC, 0.1 mM PMSF).

For srHC experiments, samples were sonicated using a Diagenode Biorupter UCD-200 (settings: 30 sec on high, 30 sec off for 30 minutes), Triton-X 100 added to 1%, debris pelleted for 15min at 4°C, and supernatant collected. DNA was extracted from 50 μL chromatin by adding 150 μL TE/1% SDS and decrosslinked overnight at 65°C. Next, 200 μL TE and 8 uL 10 mg/mL RNAse A added for 2 hours at 37°C shaking. Next, 4 μL 20 mg/mL Proteinase K was added for 2 hours at 55°C shaking. DNA was extracted by phenol:chloroform:isoamyl separation and ethanol precipitation.

For ChIP experiments, hepatocytes in AS-sonication lysis buffer proceeded to the extensive sonication and ChIP protocol in Nicetto et al., (manuscript accepted, *Science*). P14 and M2 hepatocyte H3K27me3 (Millipore 07-449) libraries were then generated using the ThruPlex DNA-seq kit (Rubicon #R400428). The M2 H3K27me3 ChIP was previously published Nicetto et al. (GSE114198).

RNA-seq

RNA was isolated using TRIzol, polyA-selected I(nvitrogen (dT)25-61002), libraries prepped (NEB 7420), and sequenced with 75 bp single-end reads. For P14 *Wt* versus *Ezh1* libraries, libraries were prepped with the NEBNext E6110.

Immunohistochemistry

Mice were prepped as for liver cannulation as described above and blood blanched from the liver with liver perfusion media. Livers were rinsed in PBS, fixed in 4% PFA-PBS for 1 hour at 4°C, washed in PBS, dehydrated, embedded in paraffin, 12 μm sections taken, dried, rehydrated in H2O, and washed. Antigen retrieval was performed in citrate buffer (10 mM Na Citrate, 0.05% Tween20, pH 6) by microwaving for 15 min. Slides were rinsed in water and PBS, quenched in 3% H2O2 in PBS for 15 min, washed, blocked for 15 min in avidin, washed, blocked for 15 min with biotin, washed, and serum blocked (10% FBS in PBS) for 30 min at room temperature. Primary antibodies were incubated in 10% FBS in PBS overnight at 4°C, washed in PBST (PBS, 0.1% Tween 20). Secondary antibodies (1/200 Santa Cruz-2004, −2005) were incubated in 10% FBS in PBS for 45 min at 37°C. Slides were washed in PBST and developed with DAB. Slides were then dehydrated and mounted with Cytoseal. PCNA antibody: 1/50 Santa Cruz 7907 Lot0402. H3K27me3 antibody: 1/500 Active Motif 39155 Lot 01613015. CK19 antibody: 1/100 from Ben Stanger's Lab. For statistics, the two-sided student's ttest with ftest were used on the average percent staining per animal.

TUNEL staining: Trevigen TACS TdT-DAB kit (Cat #4801-30-K) after avidin/biotin blocking.

H3K27me3 gene body coverage increase statistical analysis

Monte Carlo simulation was employed to assess the significance of the gene body coverage by H3K27me3 domains (Figure 1D): the selected genes were measured for a median P14-M2 increase in gene body domain coverage, a random set of genes of equal size was sampled, and the median difference in gene body domain coverage was measured 1,000

times, with the p-value estimated as the number of samples in which the median difference met or exceeded the observed difference divided by 1,000.

srHC

10 μg DNA from sonicated chromatin were resuspended in 50 μL TE. For large fragments: 25 μL beads (0.5 volumes) (Beckman Coulter A63881) were added to the 50uL of DNA, incubated, and beads were removed and large DNA isolated from them as described by the manufacturer. For medium fragments: 10 μL beads (0.2 volumes) were added to the supernatant from the large beads/DNA slurry, incubated, and beads were removed and medium DNA isolated from the beads. For small fragments: 35 μL beads (0.7 volumes) were added to the supernatant from the medium beads/DNA slurry, incubated, and beads were removed and small DNA isolated from the beads. Size selection efficacy was confirmed (Agilent 5067-4626) (Figure S3a).

For library preparation considerations, large DNA was sonicated after size selection with a Covaris S220 with the following settings PP-175 W, DF-10, CB-200, 4-9°C, 5 minutes, then ethanol precipitated.

Libraries were prepped (NEB E7370) per the manufacturer's recommendations. For size selection of small libraries: 55 μL beads for the first step and 25 μL beads for the second step. Libraries were sequenced with 75 bp single-end reads.

Enhancer-promoter unit and DHS processing

EPUs were downloaded from Shen et al, 2007[70]. 1 bp was added to enhancers that loop to multiple genes. Enhancers were centered by intersecting with concatenated liver DHS sites (GSM1014195 replicates 1-14)[71]. The first DHS event in each enhancer was used.

Domain calling

We adapted a previously described algorithm[29] to call domains. H3K27me3 parameters: 2kb windows, 1kb slide, top 30% cutoff. srHC parameters: 10kb windows, 2kb slide, and 40% cutoff. Intermediate domains include regions not called as hetero/euchromatic and heterochromatin/euchromatin double positive regions. 50% or 75% coverage by domains were used for marked gene and promoter calls, respectively.

DNA-sequencing and processing

Reads were aligned to the NCBI v37/mm9 genome using STAR2.4.2a with the following arguments: --outFilterMultimapNmax 20, --alignIntronMax 1, then filtered for unique alignments to avoid PCR duplication artifacts. RPM-normalized bedgraphs of alignments were generated, then values log2(large/small) or ChIP minus Input subtracted calculated for every block. To avoid dividing by zero, a small addend was added to every block. Biological replicate values were merged using bedtools unionbedg and averaged.

Read density (or srHC-seq scores) were calculated using the Bioconductor Genomation v1.6.0 package using ChIP minus Input (negative values converted to 0) or log2(large/small) bigwigs. The resulting values were quantile-normalized across all P14 and M2 individual

biological replicates. On box and whisker plots, whiskers indicate 5th and 95th percentiles and Wilcoxon statistical testing was used.

RNA-sequencing and processing

Reads were aligned to the mm9 genome using STAR2.4.2a with the following arguments: --outFilterType BySJout, --outFilterMultimapNmax 20, --alignSJoverhangMin 8, --alignSJDBoverhangMin 1, --outFilterMismatchNmax 999, --alignIntronMin 20, --alignIntronMax 1000000. HTSeq version 0.6.1p1 count was used to assign reads to genes with the NCBI v37/mm9 genome file (RefSeq genes, refFlat), then normalized and DE genes called using DESeq2 (alpha ≤ 0.05, FC ≥ 2).

For browser views, alignments greater that 75 bp were filtered out to avoid showing spurious intronic signal, and converted to RPM-normalized strand-specific bigWigs. Replicates were averaged at the RPM-normalized bedGraph stage with the tool bedtools unionbedg.

Zonated genes were kindly provided by Dr. Itzkovitz[72].

Experimental model and subject details

All animal studies were performed with the University of Pennsylvania IACUC approval. Genetics include the *Alb-Cre* transgene[73], and *Ezh1*$^{-/-}$[37] and *Ezh2*$^{f/f}$ (Ezh2tm1Tara)[74] alleles in a mixed C57BL/6J and C3H background.

Supplementary Material

Refer to Web version on PubMed Central for supplementary material.

Acknowledgements

We thank the Elaine Fuchs lab for the *Ezh1* mutant mice, Ryan McCarthy and Tony Hsieh for comments on the manuscript, and Bomyi Lim for help with confocal microscopy.

Grant support: This work was supported by grants by University of Pennsylvania DSRB Training Grant NIH T32HD083185-01 to J.M.G and NIH R01GM036477 to K.S.Z.

Abbreviations:

ChIP	chromatin immunoprecipitation
DHS	DNase hypersensitive sites
NAFLD	nonalcoholic fatty liver disease
NASH	nonalcoholic steohepatitis
PRC2	Polycomb Repressive Complex 2
RNA-seq	RNA-sequencing
RNAP2	RNA polymerase 2
srHC-seq	sonication-resistant heterochromatin sequencing

TSS	transcriptional start site

References

1. Horisawa K, Suzuki A. Cell-Based Regenerative Therapy for Liver Disease In: Nakao K, Minato N, Uemoto S, eds. Innovative Medicine: Basic Research and Development. Tokyo: Springer; 2015 Available at: http://www.ncbi.nlm.nih.gov/books/NBK500332/ [Accessed July 20, 2018].
2. Ieda M. Direct reprogramming into desired cell types by defined factors. Keio J Med 2013;62:74–82. [PubMed: 23801083]
3. Johannesson B, Sui L, Freytes DO, et al. Toward beta cell replacement for diabetes. EMBO J 2015;34:841–855. [PubMed: 25733347]
4. Patel V, Mathison M, Singh VP, et al. Direct Cardiac Cellular Reprogramming for Cardiac Regeneration. Curr Treat Options Cardiovasc Med 2016;18:58. [PubMed: 27554127]
5. Duan Y, Ma X, Ma X, et al. Differentiation and characterization of metabolically functioning hepatocytes from human embryonic stem cells. Stem Cells 2010;28:674–686. [PubMed: 20135682]
6. Roelandt P, Vanhove J, Verfaillie C. Directed differentiation of pluripotent stem cells to functional hepatocytes. Methods Mol Biol 2013;997:141–147. [PubMed: 23546753]
7. Si-Tayeb K, Noto FK, Nagaoka M, et al. Highly efficient generation of human hepatocyte-like cells from induced pluripotent stem cells. Hepatology 2010;51:297–305. [PubMed: 19998274]
8. Song Z, Cai J, Liu Y, et al. Efficient generation of hepatocyte-like cells from human induced pluripotent stem cells. Cell Res 2009;19:1233–1242. [PubMed: 19736565]
9. Chen Y-F, Tseng C-Y, Wang H-W, et al. Rapid generation of mature hepatocyte-like cells from human induced pluripotent stem cells by an efficient three-step protocol. Hepatology 2012;55:1193–1203. [PubMed: 22095466]
10. Huang P, He Z, Ji S, et al. Induction of functional hepatocyte-like cells from mouse fibroblasts by defined factors. Nature 2011;475:386–389. [PubMed: 21562492]
11. Huang P, Zhang L, Gao Y, He Z, et al. Direct reprogramming of human fibroblasts to functional and expandable hepatocytes. Cell Stem Cell 2014;14:370–384. [PubMed: 24582927]
12. Sekiya S, Suzuki A. Direct conversion of mouse fibroblasts to hepatocyte-like cells by defined factors. Nature 2011;475:390–393. [PubMed: 21716291]
13. Duncan AW, Dorrell C, Grompe M. Stem cells and liver regeneration. Gastroenterology 2009;137:466–481. [PubMed: 19470389]
14. Zaret KS, Grompe M. Generation and regeneration of cells of the liver and pancreas. Science 2008;322:1490–1494. [PubMed: 19056973]
15. Bhate A, Parker DJ, Bebee TW, et al. ESRP2 controls an adult splicing programme in hepatocytes to support postnatal liver maturation. Nat Commun 2015;6:8768. [PubMed: 26531099]
16. Morford LA, Davis C, Jin L, et al. The oncofetal gene glypican 3 is regulated in the postnatal liver by zinc fingers and homeoboxes 2 and in the regenerating liver by alpha-fetoprotein regulator 2. Hepatology 2007;46:1541–1547. [PubMed: 17668883]
17. Perincheri S, Dingle RWC, Peterson ML, et al. Hereditary persistence of alpha-fetoprotein and H19 expression in liver of BALB/cJ mice is due to a retrovirus insertion in the Zhx2 gene. Proc Natl Acad Sci USA 2005;102:396–401. [PubMed: 15626755]
18. Shearer MJ, Rahim S, Barkhan P, et al. Plasma vitamin K1 in mothers and their newborn babies. Lancet 1982;2:460–463. [PubMed: 6125638]
19. Avior Y, Levy G, Zimerman M, et al. Microbial-derived lithocholic acid and vitamin K2 drive the metabolic maturation of pluripotent stem cells-derived and fetal hepatocytes. Hepatology 2015;62:265–278. [PubMed: 25808545]
20. Morelli L. Postnatal development of intestinal microflora as influenced by infant nutrition. J Nutr 2008;138:1791S–1795S. [PubMed: 18716188]
21. Duncan AW. Aneuploidy, polyploidy and ploidy reversal in the liver. Semin Cell Dev Biol 2013;24:347–356. [PubMed: 23333793]

22. Koppens MAJ, Bounova G, Gargiulo G, et al. Deletion of Polycomb Repressive Complex 2 From Mouse Intestine Causes Loss of Stem Cells. Gastroenterology 2016;151:684–697.e12. [PubMed: 27342214]
23. López-Arribillaga E, Rodilla V, Pellegrinet L, et al. Bmi1 regulates murine intestinal stem cell proliferation and self-renewal downstream of Notch. Development 2015;142:41–50. [PubMed: 25480918]
24. Liu X, Wei W, Li X, et al. BMI1 and MEL18 Promote Colitis-Associated Cancer in Mice via REG3B and STAT3. Gastroenterology 2017;153:1607–1620. [PubMed: 28780076]
25. Cervantes S, Fontcuberta-PiSunyer M, Servitja J-M, et al. Late-stage differentiation of embryonic pancreatic β-cells requires Jarid2. Sci Rep 2017;7:11643. [PubMed: 28912479]
26. Xu C-R, Cole PA, Meyers DJ, et al. Chromatin "prepattern" and histone modifiers in a fate choice for liver and pancreas. Science 2011;332:963–966. [PubMed: 21596989]
27. Koike H, Ouchi R, Ueno Y, et al. Polycomb group protein Ezh2 regulates hepatic progenitor cell proliferation and differentiation in murine embryonic liver. PLoS ONE 2014;9:e104776. [PubMed: 25153170]
28. Bae WK, Kang K, Yu JH, et al. The methyltransferases enhancer of zeste homolog (EZH) 1 and EZH2 control hepatocyte homeostasis and regeneration. FASEB J 2015;29:1653–1662. [PubMed: 25477280]
29. Becker JS, McCarthy RL, Sidoli S, et al. Genomic and Proteomic Resolution of Heterochromatin and Its Restriction of Alternate Fate Genes. Mol Cell 2017;68:1023–1037.e15. [PubMed: 29272703]
30. Matoba S, Liu Y, Lu F, et al. Embryonic development following somatic cell nuclear transfer impeded by persisting histone methylation. Cell 2014;159:884–895. [PubMed: 25417163]
31. Onder TT, Kara N, Cherry A, et al. Chromatin-modifying enzymes as modulators of reprogramming. Nature 2012;483:598–602. [PubMed: 22388813]
32. Soufi A, Donahue G, Zaret KS. Facilitators and impediments of the pluripotency reprogramming factors' initial engagement with the genome. Cell 2012;151:994–1004. [PubMed: 23159369]
33. Sridharan R, Gonzales-Cope M, Chronis C, et al. Proteomic and genomic approaches reveal critical functions of H3K9 methylation and heterochromatin protein-1γ in reprogramming to pluripotency. Nat Cell Biol 2013;15:872–882. [PubMed: 23748610]
34. Belayew A, Tilghman SM. Genetic analysis of alpha-fetoprotein synthesis in mice. Mol Cell Biol 1982;2:1427–1435. [PubMed: 6186903]
35. Boyer LA, Plath K, Zeitlinger J, et al. Polycomb complexes repress developmental regulators in murine embryonic stem cells. Nature 2006;441:349–353. [PubMed: 16625203]
36. Ezhkova E, Lien W-H, Stokes N, et al. EZH1 and EZH2 cogovern histone H3K27 trimethylation and are essential for hair follicle homeostasis and wound repair. Genes Dev 2011;25:485–498. [PubMed: 21317239]
37. Margueron R, Li G, Sarma K, et al. Ezh1 and Ezh2 maintain repressive chromatin through different mechanisms. Mol Cell 2008;32:503–518. [PubMed: 19026781]
38. Shen X, Liu Y, Hsu Y-J, et al. EZH1 mediates methylation on histone H3 lysine 27 and complements EZH2 in maintaining stem cell identity and executing pluripotency. Mol Cell 2008;32:491–502. [PubMed: 19026780]
39. Gopal E, Miyauchi S, Martin PM, et al. Expression and functional features of NaCT, a sodium-coupled citrate transporter, in human and rat livers and cell lines. Am J Physiol Gastrointest Liver Physiol 2007;292:G402–408. [PubMed: 16973915]
40. Ruscica M, Ferri N, Macchi C, et al. Liver fat accumulation is associated with circulating PCSK9. Ann Med 2016;48:384–391. [PubMed: 27222915]
41. Thatcher JE, Zelter A, Isoherranen N. The relative importance of CYP26A1 in hepatic clearance of all-trans retinoic acid. Biochem Pharmacol 2010;80:903–912. [PubMed: 20513361]
42. Conforto TL, Zhang Y, Sherman J, et al. Impact of CUX2 on the female mouse liver transcriptome: activation of female-biased genes and repression of male-biased genes. Mol Cell Biol 2012;32:4611–4627. [PubMed: 22966202]
43. Simon JA, Kingston RE. Mechanisms of polycomb gene silencing: knowns and unknowns. Nat Rev Mol Cell Biol 2009;10:697–708. [PubMed: 19738629]

44. Beisel C, Paro R. Silencing chromatin: comparing modes and mechanisms. Nat Rev Genet 2011;12:123–135. [PubMed: 21221116]
45. Breiling A, Turner BM, Bianchi ME, et al. General transcription factors bind promoters repressed by Polycomb group proteins. Nature 2001;412:651–655. [PubMed: 11493924]
46. Dellino GI, Schwartz YB, Farkas G, et al. Polycomb silencing blocks transcription initiation. Mol Cell 2004;13:887–893. [PubMed: 15053881]
47. Hawkins RD, Hon GC, Lee LK, et al. Distinct epigenomic landscapes of pluripotent and lineage-committed human cells. Cell Stem Cell 2010;6:479–491. [PubMed: 20452322]
48. Ku M, Koche RP, Rheinbay E, et al. Genomewide analysis of PRC1 and PRC2 occupancy identifies two classes of bivalent domains. PLoS Genet 2008;4:e1000242. [PubMed: 18974828]
49. Trojer P, Reinberg D. Facultative heterochromatin: is there a distinctive molecular signature? Mol Cell 2007;28:1–13. [PubMed: 17936700]
50. Jadhav U, Nalapareddy K, Saxena M, et al. Acquired Tissue-Specific Promoter Bivalency Is a Basis for PRC2 Necessity in Adult Cells. Cell 2016;165:1389–1400. [PubMed: 27212235]
51. Alpern D, Langer D, Ballester B, et al. TAF4, a subunit of transcription factor II D, directs promoter occupancy of nuclear receptor HNF4A during post-natal hepatocyte differentiation. Elife 2014;3:e03613. [PubMed: 25209997]
52. van Koppen A, Verschuren L, van den Hoek AM, et al. Uncovering a Predictive Molecular Signature for the Onset of NASH-Related Fibrosis in a Translational NASH Mouse Model. Cell Mol Gastroenterol Hepatol 2018;5:83–98.e10. [PubMed: 29276754]
53. Teufel A, Itzel T, Erhart W, et al. Comparison of Gene Expression Patterns Between Mouse Models of Nonalcoholic Fatty Liver Disease and Liver Tissues From Patients. Gastroenterology 2016;151:513–525.e0. [PubMed: 27318147]
54. Ramnath D, Irvine KM, Lukowski SW, et al. Hepatic expression profiling identifies steatosis-independent and steatosis-driven advanced fibrosis genes. JCI Insight 2018;3.
55. Ippolito DL, AbdulHameed MDM, Tawa GJ, et al. Gene Expression Patterns Associated With Histopathology in Toxic Liver Fibrosis. Toxicol Sci 2016;149:67–88. [PubMed: 26396155]
56. Murphy N, Gaynor KU, Rowan SC, et al. Altered Expression of Bone Morphogenetic Protein Accessory Proteins in Murine and Human Pulmonary Fibrosis. Am J Pathol 2016;186:600–615. [PubMed: 26765958]
57. Dattaroy D, Pourhoseini S, Das S, et al. Micro-RNA 21 inhibition of SMAD7 enhances fibrogenesis via leptin-mediated NADPH oxidase in experimental and human nonalcoholic steatohepatitis. Am J Physiol Gastrointest Liver Physiol 2015;308:G298–312. [PubMed: 25501551]
58. Choi SS, Diehl AM. Epithelial-to-mesenchymal transitions in the liver. Hepatology 2009;50:2007–2013. [PubMed: 19824076]
59. Cui JY, Renaud HJ, Klaassen CD. Ontogeny of novel cytochrome P450 gene isoforms during postnatal liver maturation in mice. Drug Metab Dispos 2012;40:1226–1237. [PubMed: 22446519]
60. Fouts JR, Adamson RH. Drug metabolism in the newborn rabbit. Science 1959;129:897–898. [PubMed: 13635031]
61. Treluyer JM, Cheron G, Sonnier M, et al. Cytochrome P-450 expression in sudden infant death syndrome. Biochem Pharmacol 1996;52:497–504. [PubMed: 8687505]
62. Wong MCS, Huang J. The growing burden of liver cirrhosis: implications for preventive measures. Hepatol Int 2018;12:201–203. [PubMed: 29679258]
63. Jung YK, Yim HJ. Reversal of liver cirrhosis: current evidence and expectations. Korean J Intern Med 2017;32:213–228. [PubMed: 28171717]
64. Chopra VS, Hong J-W, Levine M. Regulation of Hox gene activity by transcriptional elongation in Drosophila. Curr Biol 2009;19:688–693. [PubMed: 19345103]
65. Tie F, Banerjee R, Fu C, et al. Polycomb inhibits histone acetylation by CBP by binding directly to its catalytic domain. Proc Natl Acad Sci USA 2016;113:E744–753. [PubMed: 26802126]
66. Ardehali MB, Anselmo A, Cochrane JC, et al. Polycomb Repressive Complex 2 Methylates Elongin A to Regulate Transcription. Mol Cell 2017;68:872–884.e6. [PubMed: 29153392]

67. Nitta T, Kim J-S, Mohuczy D, et al. Murine cirrhosis induces hepatocyte epithelial mesenchymal transition and alterations in survival signaling pathways. Hepatology 2008;48:909–919. [PubMed: 18712785]

68. Dooley S, Hamzavi J, Ciuclan L, et al. Hepatocyte-specific Smad7 expression attenuates TGF-beta-mediated fibrogenesis and protects against liver damage. Gastroenterology 2008;135:642–659. [PubMed: 18602923]

69. Taura K, Miura K, Iwaisako K, et al. Hepatocytes do not undergo epithelial-mesenchymal transition in liver fibrosis in mice. Hepatology 2010;51:1027–1036. [PubMed: 20052656]

70. Shen Y, Yue F, McCleary DF, et al. A map of the cis-regulatory sequences in the mouse genome. Nature 2012;488:116–120. [PubMed: 22763441]

71. Yue F, Cheng Y, Breschi A, Vierstra A, Wu W, Ryba T, Sandstrom R, Ma Z, Davis C, Pope B, Shen Y, et al. A comparative encyclopedia of DNA elements in the mouse genome. Nature 2014;515:355–364. [PubMed: 25409824]

72. Halpern KB, Shenhav R, Matcovitch-Natan O, et al. Single-cell spatial reconstruction reveals global division of labour in the mammalian liver. Nature 2017;542:352–356. [PubMed: 28166538]

73. Postic C, Shiota M, Niswender KD, et al. Dual roles for glucokinase in glucose homeostasis as determined by liver and pancreatic beta cell-specific gene knock-outs using Cre recombinase. J Biol Chem 1999;274:305–315. [PubMed: 9867845]

74. Su I-H, Basavaraj A, Krutchinsky AN, et al. Ezh2 controls B cell development through histone H3 methylation and Igh rearrangement. Nat Immunol 2003;4:124–131. [PubMed: 12496962]

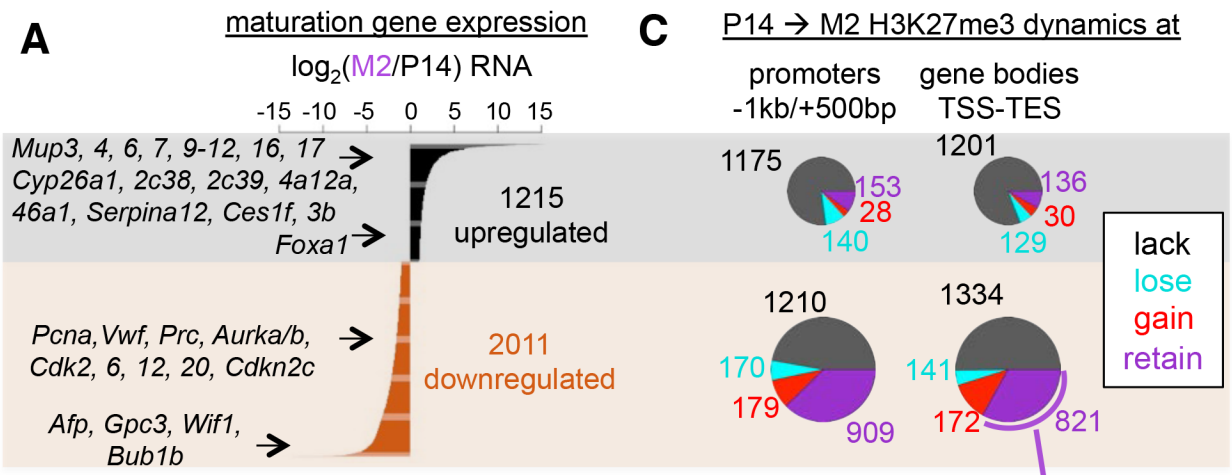

B

gene ontology

	term	# genes	enrichment	FDR
1215	liver	371	1.8	2E-30
	metabolic pathways	162	2.1	5E-19
	transport	128	1.3	5E+00
	oxidation-reduction process	94	2.5	4E-13
	lipid metabolic process	63	2.5	9E-08
	retinol metabolism	37	6.8	4E-18
	xenobiotic metab by cytochrome P450	33	8.4	2E-19
	bile secretion	14	3.2	4E-01
	primary bile acid biosynthesis	6	6.1	3E+00
2011	cell cycle	146	2.5	4E-23
	multicellular organism development	128	1.3	2E+00
	cell adhesion	125	2.7	1E-22
	cell differentiation	98	1.3	5E+00
	protein phosphorylation	85	1.6	6E-02
	PI3K-Akt signaling pathway	60	1.8	1E-02
	Focal adhesion	56	2.8	7E-10
	ECM-receptor interaction	41	4.9	1E-15

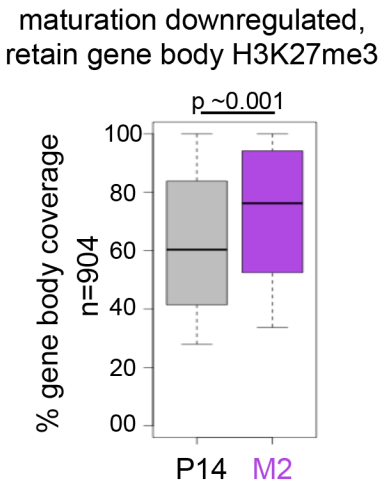

Figure 1. Postnatal hepatic maturation during the P14 to M2 transition involves differential expression of thousands of genes and H3K27me3 dynamics.

(A) $\log_2$(M2/P14 fold change) for genes differentially expressed in maturing hepatocytes.

(B) Gene Ontology for genes up and downregulated from P14 to M2 in *Wt* hepatocytes.

(C) H3K27me3 dynamics at genes up- (top, grey shading) and downregulated (bottom, orange shading) in maturation

(D) Percent H3K27me3 gene body coverage of "retain" H3K27me3 genes. Monte Carlo simulation and estimated p-value. Whiskers: 5^{th}/95^{th} percentiles.

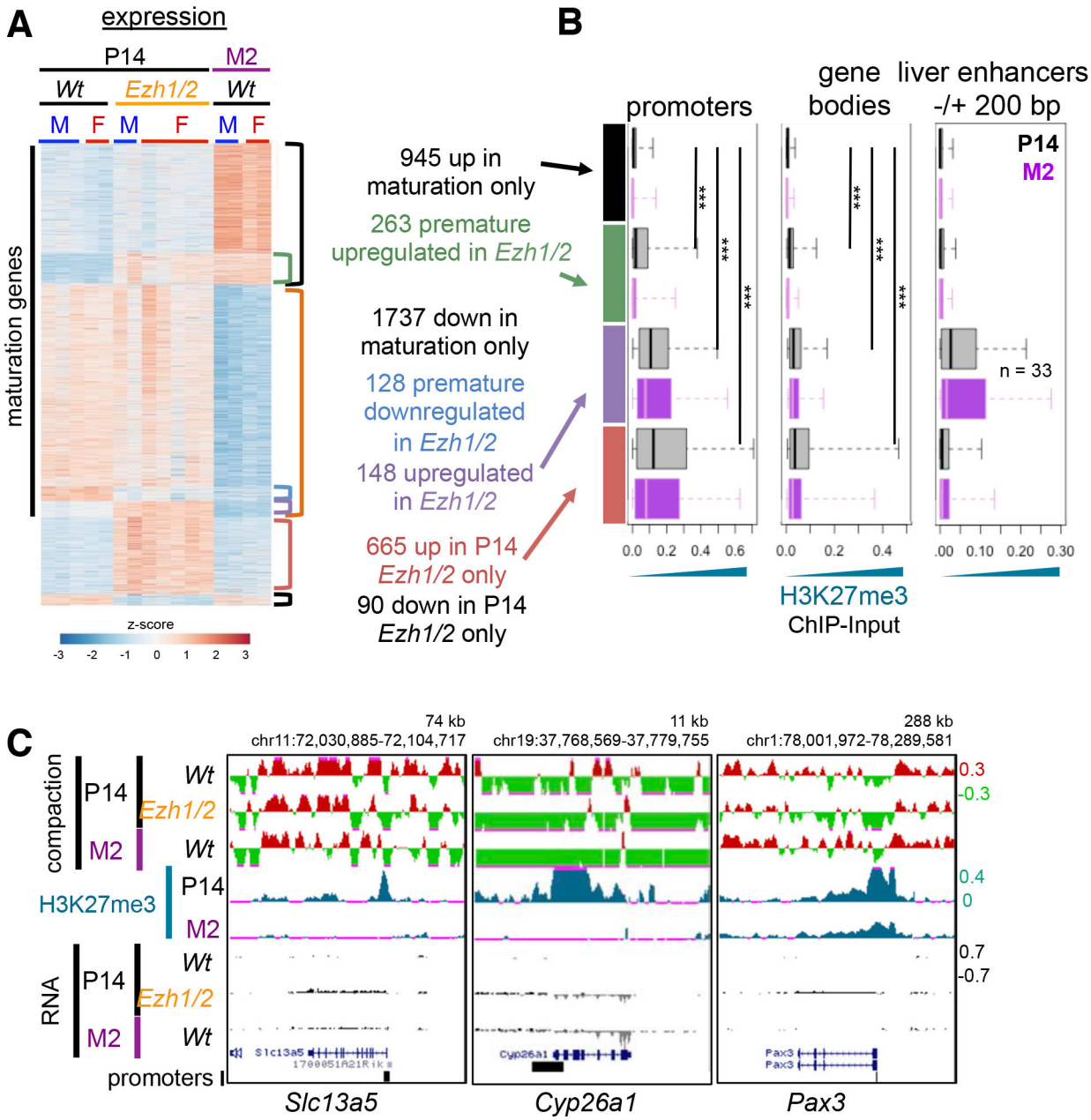

Figure 2. PRC2 proteins EZH1/2 restrain postnatal hepatic maturation.

(A) Relative expression of genes differentially expressed in maturation or in P14 *Ezh1/2* hepatocytes.

(B) P14 and M2 H3K27me3 density at promoters, genes, or enhancers. Whiskers: 5th/95th percentiles. Wilcoxon rank-sum test.

(C) srHC-seq (heterochromatic-enriched in red, euchromatic-enriched in green), H3K27me3, and RNA signal at genes prematurely upregulated in P14 *Ezh1/2* hepatocytes (*Slc15a5, Cyp26a*) and a control gene (*Pax3*).

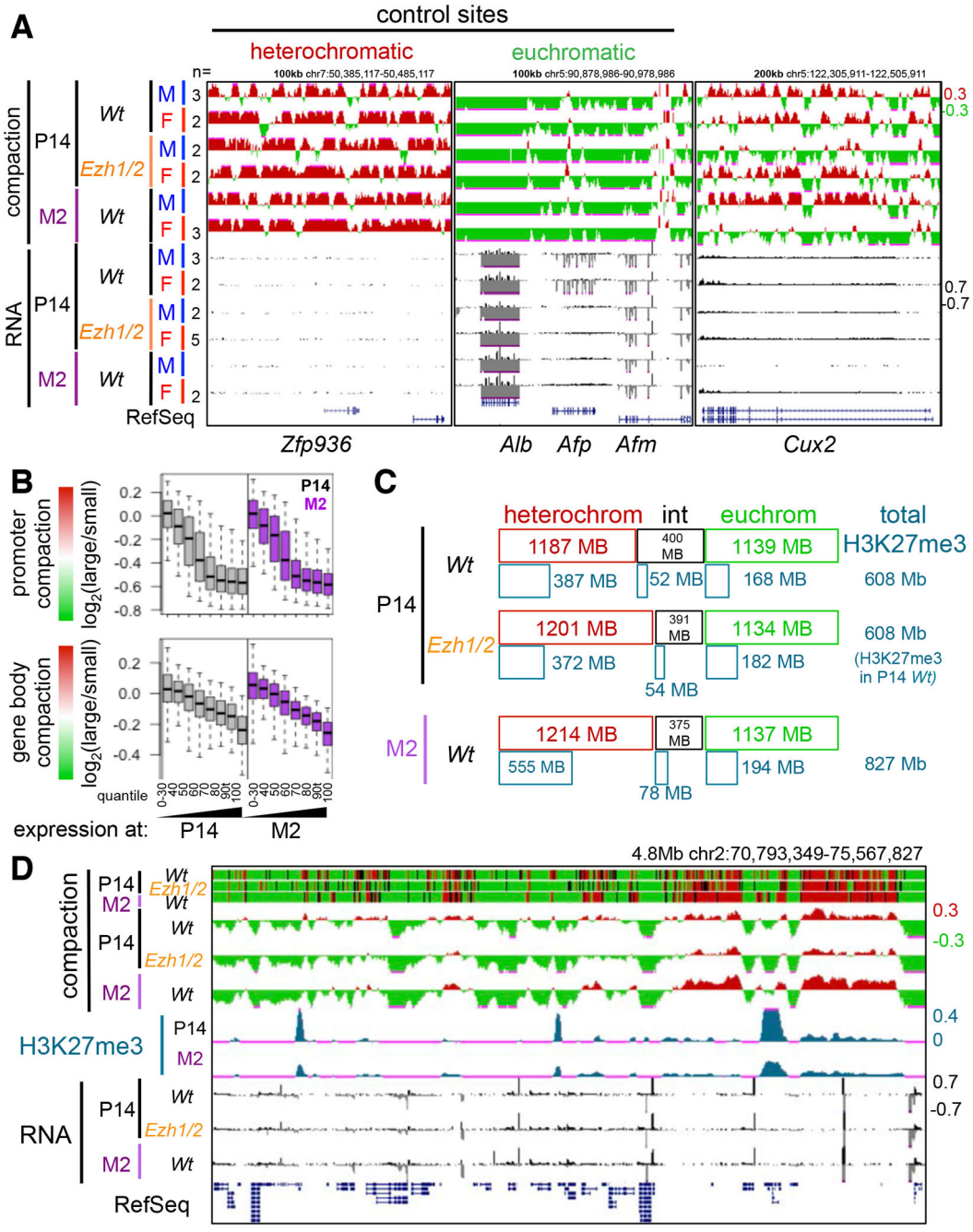

Figure 3. Stable global chromatin compaction in maturation and P14 *Ezh1/2*

(A)srHC-seq and RNA signal for positive controls sites for heterochromatin, *Zfp936*, euchromatin, *Alb* locus, or a dynamic gene, *Cux2*.

(B) srHC-seq scores at promoters and gene bodies for genes binned into expression quantiles. 0-30 represents genes without any RNA signal. Note the with increasing expression, srHC scores become more euchromatic. Whiskers: 5th/95th percentiles.

(C) Megabases of the genome called as heterochromatic, intermediate, or euchromatic and the overlap with H3K27me3 domains.

(D) srHC-seq domains and signal, H3K27me3, and RNA. Note that H3K27me3 occurs in both heterochromatic (red) and euchromatic (green) regions.

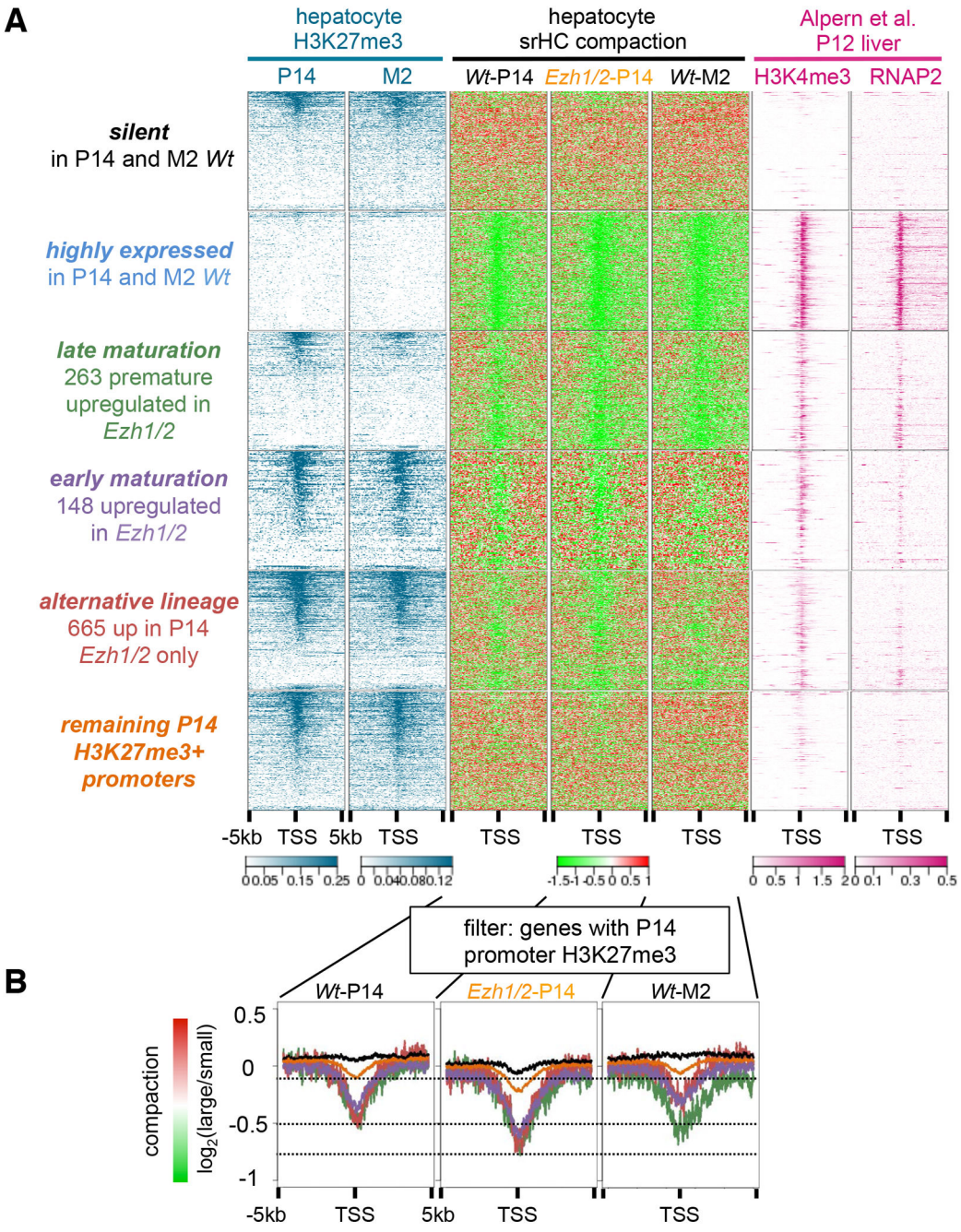

Figure 4. srHC-seq reveals that *Ezh1/2* sensitive genes have euchromatic and bivalently-marked promoters

(A) ChIP and srHC-Seq signal around transcriptional start sites (−/+ 5kb) for silent genes, genes highly expressed in P14 and M2 (top 10% in expression in P14 and M2), three classes genes upregulated in P14 *Ezh1/2*, and the remaining P14 H3K27me3+ promoters. Note that the three classes of genes upregulated in P14 *Ezh1/2* hepatocytes have euchromatic promoters (green srHC signal) in P14 *Wt* hepatocytes. In comparison promoters that have H3K27me3 but are not upregulated (bottom, orange) have heterochromatic signals (red srHC signal) in P14 *Wt* hepatocytes.

(B) srHC-seq metaplots for panel (A) groups except highly expressed genes. Filtered for genes with P14 H3K27me3-marked promoters. Note that late maturation genes, early maturation genes, and alternative lineage genes (green, purple, and red lines) have more euchromatic signal in P14 *Wt* hepatocytes than the genes which are not upregulated in P14 *Ezh1/2* and have H3K27me3+ promoters (orange line).

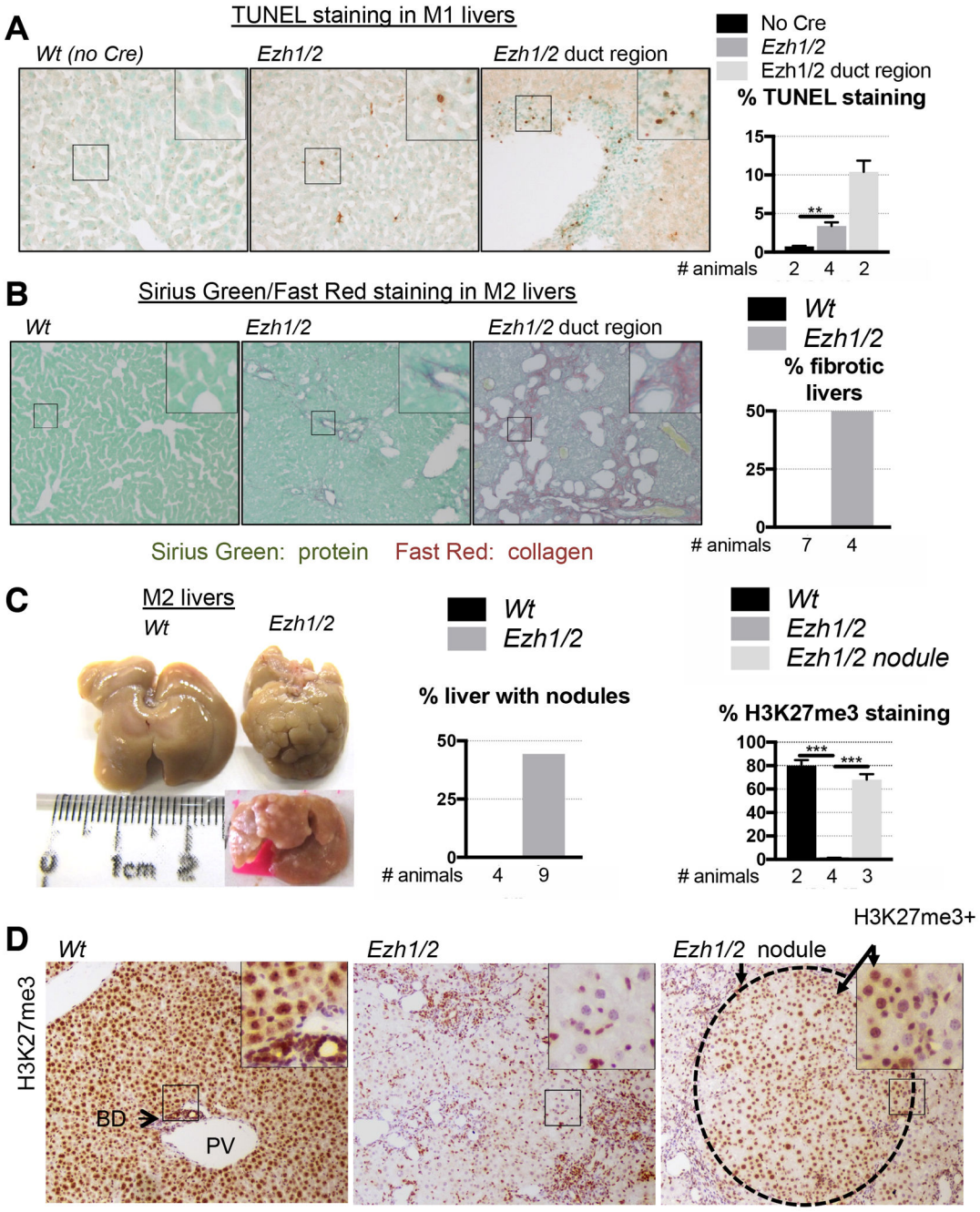

Figure 5. Ezh1/2 loss leads to chronic liver damage.

(A) Apoptosis as assayed by TUNEL staining.

(B) Fibrosis as assayed Sirius Green (total protein) and Fast Red (collagen) staining.

(C) Examples of a normal *Wt* liver and 2 *Ezh1/2* livers with macroscopic liver nodules. Quantification of animals with liver nodules as assessed by histology.

(D)H3K27me3 immunohistochemistry in M2 livers. Regions inside and outside of regenerative nodules are outlined by the dotted circle. Wt: 2034 hepatocytes counted. *Ezh1/2*: 2440 hepatocytes counted. *Ezh1/2* nodule: 1056 cells counted in 7 nodules. Two-sided student's t-test with standard error.

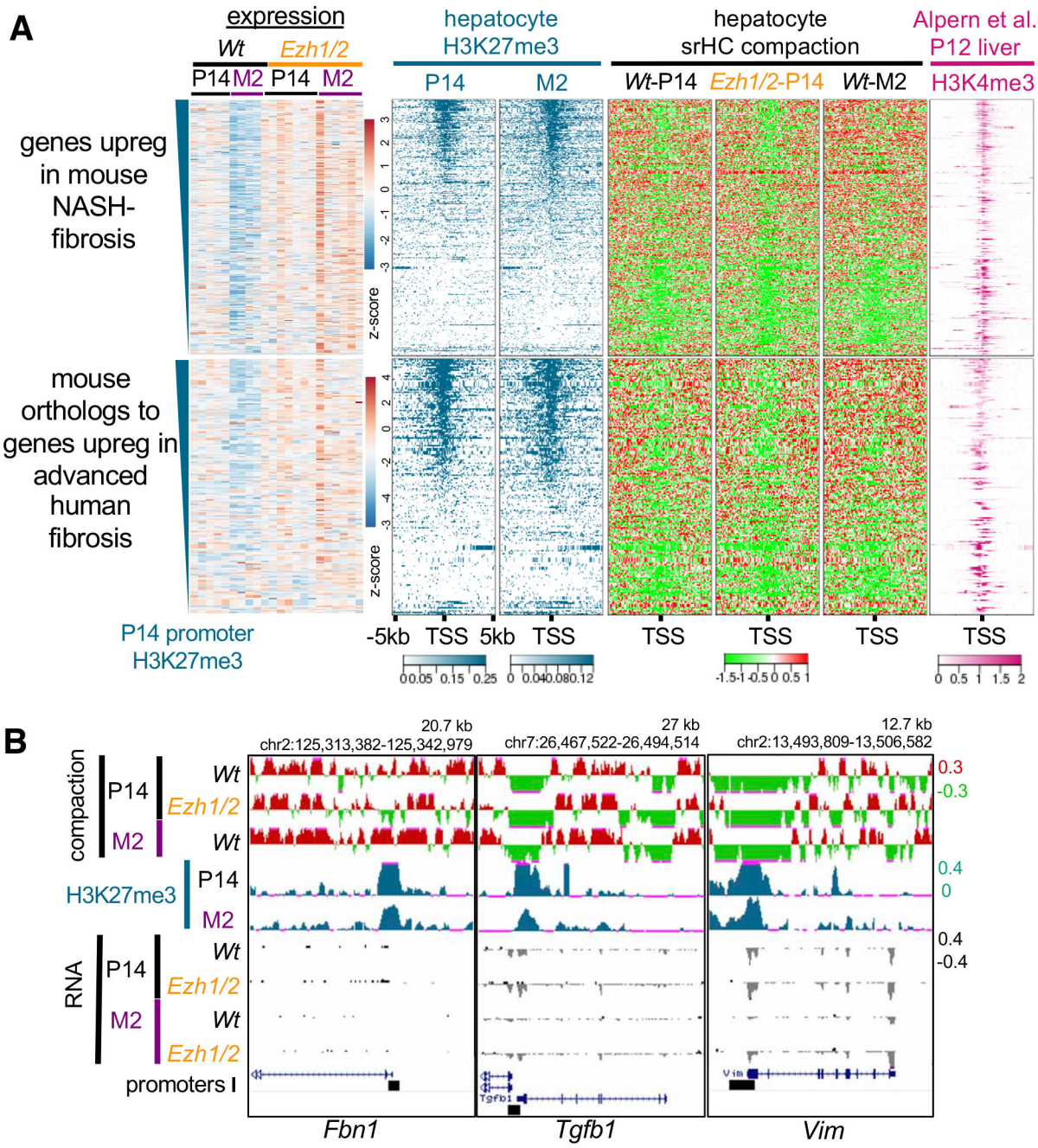

Figure 6. PRC2 represses liver fibrosis signature genes

(A) Genes upregulated in a murine model of NASH-related fibrosis (top) and genes upregulated in human advanced fibrosis patients as compared to low level fibrosis (bottom). Murine hepatocyte expression, H3K27me3 and srHC-seq, and H3K4me3 signal around transcriptional start sites −/+ 5 kb. Note that many fibrosis genes have H3K27me3+ promoters that are also euchromatic (green srHC signal) and have promoter H3K4me3. M2 *Ezh1/2* RNA-seq represents a mix of hepatocytes from inside and outside of nodules.

(B) srHC-seq, H3K27me3, and RNA signal at fibrosis-related or EMT-related genes.